

DOI: 10.1002/cmdc.201300217

## VIP Discovery of NVP-LEQ506, a Second-Generation Inhibitor of Smoothed

Stefan Peukert,\* Feng He, Miao Dai, Rui Zhang, Yingchuan Sun, Karen Miller-Moslin, Michael McEwan, Bharat Lagu, Kate Wang, Naeem Yusuff, Aaron Bourret, Arun Ramamurthy, Wieslawa Maniara, Adam Amaral, Anthony Vattay, Anlai Wang, Ribo Guo, Jing Yuan, John Green, Juliet Williams, Silvia Buonamici, Joseph F. Kelleher, III, and Marion Dorsch<sup>[a]</sup>

The Hedgehog (Hh) pathway plays an important role in embryonic development and tissue patterning and a lesser role in adults for tissue maintenance and repair.<sup>[1,2]</sup> Smoothed (Smo), a 7-pass transmembrane receptor with a GPCR-like architecture, is a key component of the Hh signaling pathway, the activity of which is suppressed by the 12-pass transmembrane protein Patched (Ptch).<sup>[3]</sup> Binding of secreted proteins of the Hh family to Ptch results in relief of the suppression of Smo, initiating downstream signaling and activation of Gli transcription factors which lead to cell proliferation, differentiation and survival. Genetic activation of the Hh pathway, mostly by Ptch loss-of-function or Smo gain-of-function mutations, has been linked to tumorigenesis in cancers such as basal cell carcinoma (BCC) and medulloblastoma.<sup>[4,5]</sup> Furthermore, up-regulation of the pathway has been linked to tumor growth in pancreatic, prostate, lung, colorectal, bladder, and ovarian cancers.<sup>[6]</sup> Recently, Smo-dependent non-canonical signaling through a Ca<sup>2+</sup>-Ampk axis has been implicated in stimulating glucose uptake, resulting in Warburg-like metabolism in muscle and brown fat.<sup>[7]</sup> Smo antagonists such as vismodegib/GDC-0449 (**1**)<sup>[8,9]</sup> and sonidegib/NVP-LDE225 (**2**)<sup>[10]</sup> have demonstrated clinical response in patients with BCC and medulloblastoma.<sup>[11,12]</sup> Vismodegib was approved in January 2012 by the US Food and Drug Administration (FDA) for the treatment of adults with metastatic or locally advanced BCC.<sup>[13]</sup> However, micromolar concentrations are required in preclinical models for efficacy,<sup>[14,15]</sup> and in at least one patient, loss of efficacy occurred from a single point mutation in Smo that prevented the binding of **1**.<sup>[16]</sup> Furthermore, adverse events of muscle spasms and weight loss occurred in > 50% of the patients,<sup>[17]</sup> possibly related to activation of non-canonical Hh signaling.<sup>[7]</sup> Thus, our efforts for a second-generation Smo antagonist were directed

toward the identification of compounds with further improved potency to achieve optimal efficacy.

Based on our previously published 1-amino-4-benzylphthalazine **3a**,<sup>[18]</sup> we aimed for compounds with better potency, decreased hERG activity, and improved aqueous solubility by truncating the bicyclic phthalazine core to yield compounds of general structure **4** (Figure 1). Herein we describe our research

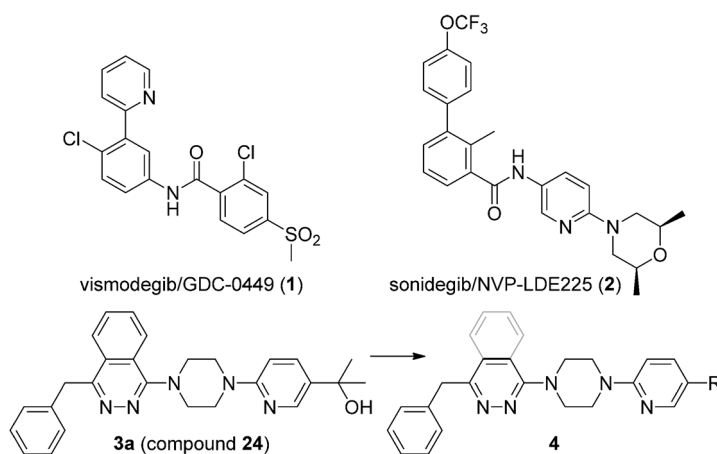


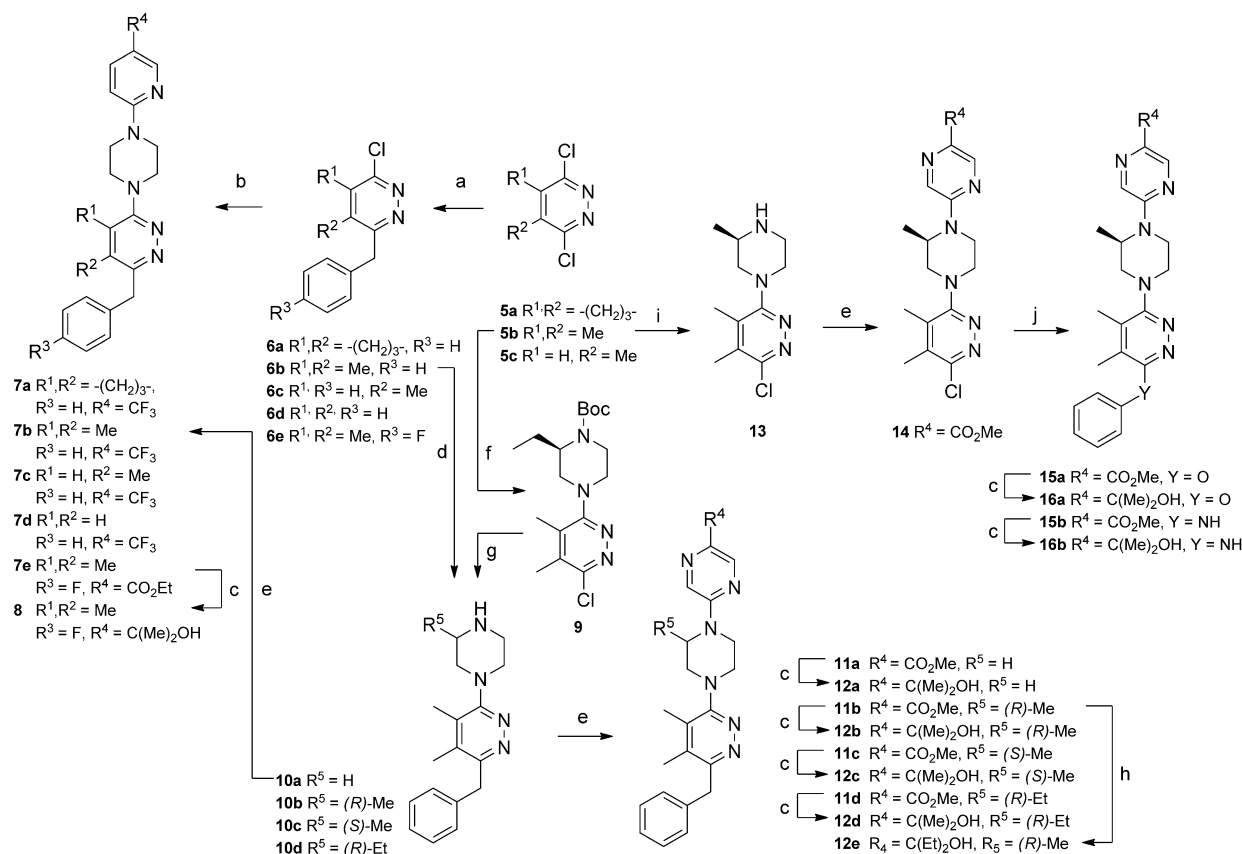
**Figure 1.** Structures of vismodegib, sonidegib, and the strategy used to identify pyridazines **4** based on the previously reported lead compound **3a**.

resulting in the discovery of NVP-LEQ506 (**12b**) which is currently in clinical development.

The preparation and characterization of phthalazines **3** has been previously described,<sup>[18]</sup> while compounds of general structure **4** were synthesized by starting from readily available 3,6-dichloropyridazines **5** (Scheme 1). In the first route, Negishi coupling<sup>[19]</sup> with benzylzinc bromides provided the mono-chloro intermediates **6** which reacted under thermal conditions with *N*-arylpiperazines to yield compounds **7**. Intermediate **6b** was converted with excess piperazines to afford compounds **10a–c**. Piperazines with an alkyl substituent at the 2-position selectively afforded the regioisomers **10b,c** depicted in Scheme 1. Compound **10d** was prepared with the synthetic steps reversed: First, **5b** was heated in the presence of *N*-Boc-(*R*)-2-ethylpiperazine to yield intermediate **9**, which was then submitted to Negishi coupling with benzylzinc bromide to afford **10d** after removal of the Boc protecting group. All compounds **10** were subsequently treated with methyl 5-chloro-

[a] Dr. S. Peukert, Dr. F. He, M. Dai, R. Zhang, Y. Sun, Dr. K. Miller-Moslin, M. McEwan, Dr. B. Lagu, K. Wang, Dr. N. Yusuff, A. Bourret, A. Ramamurthy, Dr. W. Maniara, A. Amaral, A. Vattay, A. Wang, R. Guo, J. Yuan, J. Green, Dr. J. Williams, Dr. S. Buonamici, Dr. J. F. Kelleher, III, Dr. M. Dorsch  
Novartis Institutes for Biomedical Research (NIBR)  
250 Massachusetts Avenue, Cambridge, MA 02139 (USA)  
E-mail: stefan.peukert@novartis.com

Supporting information for this article is available on the WWW under <http://dx.doi.org/10.1002/cmdc.201300217>.



**Scheme 1.** Synthesis of pyridazines. *Reagents and conditions:* a) benzylzinc bromide, Pd(PPh<sub>3</sub>)<sub>4</sub>, THF, 50–65 °C; b) 1-aryl piperazine, Et<sub>3</sub>N, NMP, 190–210 °C, microwave; c) MeMgBr or MeMgI, THF, –78 °C → RT; d) piperazine, Et<sub>3</sub>N, dioxane, NMP, 190 °C, microwave; e) chloro arene, Et<sub>3</sub>N, dioxane, 80 °C or NMP, 190 °C, microwave; f) *N*-Boc-(*R*)-2-ethyl piperazine, K<sub>2</sub>CO<sub>3</sub>, DMF, 60 °C; g) 1. a), 2. TFA, CH<sub>2</sub>Cl<sub>2</sub>; h) EtMgI, THF, –78 °C → RT; i) (*R*)-2-methyl piperazine, K<sub>2</sub>CO<sub>3</sub>, DMF, 50 °C; j) **15a**: phenol, K<sub>3</sub>PO<sub>4</sub>, tBu-XPhos, toluene, 100 °C; **15b**: aniline, 190 °C, microwave.

pyridazine-2-carboxylate to provide esters **11**. Intermediate **13** was prepared by the reaction of (*R*)-2-methylpiperazine with 3,6-dichloropyridazine **5b**. Compound **14** was generated by thermal reaction of **13** with methyl 5-chloropyridazine-2-carboxylate. The phenoxy substituent in compound **15a** was installed under palladium catalysis,<sup>[20]</sup> whereas the aniline was introduced in low yield to afford compound **15b** in a non-catalyzed transformation. Tertiary alcohols **8**, **12**, and **16** were all prepared from the corresponding methyl esters by reaction with excess MeMgBr/I or EtMgI.

All compounds were evaluated in a cell-based reporter gene assay for their ability to inhibit the Hh pathway. The ability of compounds to inhibit pathway activity in a mouse cell line (TM3) was tested by competition with a Smo agonist at two different concentrations: 1 and 25 nM. A shift to a higher IC<sub>50</sub> at the higher agonist concentration in the TM3-Gli-luc IC<sub>50</sub> assay ("Gli shift") suggested antagonism of Smo.

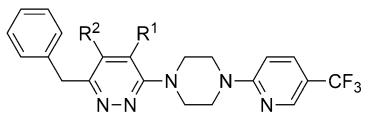
Our initial attempts to increase aqueous solubility and decrease hERG activity while maintaining the good potency of **3a** focused on the substituent R<sup>1</sup> (Table 1). However, various approaches, as represented by examples **3b–d**, were unsuccessful

**Table 1.** Smo antagonism, solubility, and hERG activity of phthalazines **3**.

Compd	R <sup>1</sup>	Gli shift [nM] <sup>[a]</sup>		Sol. [μM] <sup>[b]</sup>	hERG IC <sub>50</sub> [μM] <sup>[c]</sup>
		1 nM	25 nM		
<b>3a</b>	C(CH <sub>3</sub> ) <sub>2</sub> OH	3	35	< 5	1.5
<b>3b</b>	C(CH <sub>3</sub> ) <sub>2</sub> NH <sub>2</sub>	1	42	731	1.4
<b>3c</b>	CO <sub>2</sub> H	2665	> 5000	25	> 30
<b>3d</b>	C(CH <sub>2</sub> OH)(CH <sub>3</sub> )OH	17	136	33	8.8

[a] See the Supporting Information for a detailed description of the assay. [b] Aqueous equilibrium solubility at pH 6.8. [c] Values determined in a [<sup>3</sup>H]dofetilide hERG binding assay.

in achieving both goals simultaneously: Basic ionizable substituents led to potent hERG inhibition (compound **3b**), whereas acidic ionizable groups resulted in loss of potency (compound **3c**). Polar substituents, as exemplified by compound **3d**, typically resulted in a moderate improvement in hERG inhibition, but also in decreased Smo potency. Therefore, we pursued the idea of truncating the phthalazine core, which

**Table 2.** Smo antagonism of phthalazine **3e** versus pyridazines **7**.


Compd	R <sup>1</sup>	R <sup>2</sup>	Gli shift [nM] <sup>[a]</sup>	
			1 nM	25 nM
<b>3e</b>	benzo		134	1327
<b>7a</b>	-(CH <sub>2</sub> ) <sub>3</sub> -		97	508
<b>7b</b>	CH <sub>3</sub>	CH <sub>3</sub>	90	733
<b>7c</b>	H	CH <sub>3</sub>	251	> 5000
<b>7d</b>	H	H	> 5000	> 5000

[a] See the Supporting Information for a detailed description of the assay.

we suspected to be a contributor to the low aqueous solubility of **3a**. Table 2 shows structure–activity relationships developed for pyridazines **7a–d** in comparison with phthalazine **3e**. Replacement of the annelated benzene ring with either a cyclopentyl ring or two methyl groups afforded compounds with similar or better potency than the original phthalazine (compounds **7a,b**). A further decrease in the size of the pyridazine substituents R<sup>1</sup> and R<sup>2</sup> was not tolerated, as demonstrated with compounds **7c** and **7d**. We used compound **7b**, with its increased ligand efficiency over **3e**, as a starting point for a systematic optimization of this new scaffold (Table 3). Installment of the 2-hydroxypropyl group (compound **8**) resulted in good potency, but the compound still suffered from low aqueous solubility and potent hERG activity. Replacement of the 2-pyridyl ring with a 2-pyrazine ring afforded very good potency with improved solubility and no significant binding to the hERG channel (compound **12a**). We retained the 2-pyrazine ring and focused further optimization on the piperazine substituents. A methyl substituent on the piperazine linker resulted in a further increase in aqueous solubility (compound **12b** vs. **12a**). Improved solubility was observed despite an overall

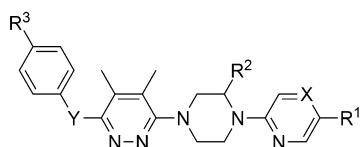
increase in lipophilicity for **12b** relative to **12a** (clogP=3.1 and 2.6 for **12b** and **12a**), and we attribute this finding to the lower melting point of **12b** relative to that of **12a** (132 vs. 161 °C). The *R* enantiomer **12b** is ~2-fold more potent than the *S* enantiomer **12c**. An analysis of several enantiomeric pairs shows that the *R*-configured R<sup>2</sup> enantiomers are consistently more potent than the corresponding *S*-configured R<sup>2</sup> enantiomer (data not shown). Further increase in steric bulk for either substituents R<sup>2</sup> or R<sup>1</sup> is detrimental for the aqueous solubility of the compounds (compounds **12d** and **e**) and does not provide any additional gain in potency. Notably, replacement of the benzylic methylene linker with an oxygen atom (compound **16a**) is well tolerated, whereas replacement with an NH group (compound **16b**) results in a ~10-fold decrease in inhibition of the Hh pathway. These two compounds demonstrate the sensitive nature of the structure–solubility relationship. Despite increases in polar surface areas for both compounds **16a** and **16b** relative to **12b** (87.3, 90.3, and 78.3 Å for **16a**, **b**, and **12b**) a drop in solubility is observed.<sup>[21]</sup>

Overall, compound **12b** provided the best combination of excellent potency in the Gli-luc assay, low hERG channel binding, which was substantiated in an automated patch clamp assay, and acceptable aqueous solubility to minimize the potential for solubility-limited absorption. Therefore, **12b** was selected for a detailed in vitro evaluation (Table 4). Binding assays, using both human and mouse receptor, confirmed that **12b** targets Smo within the Hh pathway and binds to both re-

**Table 4.** In vitro potency of **12b** in comparison with **2**.<sup>[a]</sup>

Compd	IC <sub>50</sub> [nM]			
	human Smo	mouse Smo	HEPM <sup>[b]</sup>	Smo D473H
<b>12b</b>	2	4	2	96
<b>2</b>	11	12	13	–

[a] See the Supporting Information for detailed descriptions of all assays.  
[b] HEPM = human embryonic palatal mesenchymal.

**Table 3.** Smo antagonism, solubility, and hERG activity of pyridazines **8**, **12**, and **16**.


Compd	R <sup>1</sup>	R <sup>2</sup>	R <sup>3</sup>	X	Y	Gli shift [nM] <sup>[a]</sup>		Sol. [μM] <sup>[b]</sup>	hERG IC <sub>50</sub> [μM] <sup>[c]</sup>
						1 nM	25 nM		
<b>8</b>	C(CH <sub>3</sub> ) <sub>2</sub> OH	H	F	CH	CH <sub>2</sub>	5	76	< 5	1.3
<b>12a</b>	C(CH <sub>3</sub> ) <sub>2</sub> OH	H	H	N	CH <sub>2</sub>	2	60	11	> 30
<b>12b</b>	C(CH <sub>3</sub> ) <sub>2</sub> OH	( <i>R</i> )-CH <sub>3</sub>	H	N	CH <sub>2</sub>	1	10	34	30
<b>12c</b>	C(CH <sub>3</sub> ) <sub>2</sub> OH	( <i>S</i> )-CH <sub>3</sub>	H	N	CH <sub>2</sub>	2	34	–	–
<b>12d</b>	C(CH <sub>3</sub> ) <sub>2</sub> OH	( <i>R</i> )-CH <sub>2</sub> CH <sub>3</sub>	H	N	CH <sub>2</sub>	4	57	7	> 30
<b>12e</b>	C(CH <sub>2</sub> CH <sub>3</sub> ) <sub>2</sub> OH	( <i>R</i> )-CH <sub>3</sub>	H	N	CH <sub>2</sub>	1	18	< 5	–
<b>16a</b>	C(CH <sub>3</sub> ) <sub>2</sub> OH	( <i>R</i> )-CH <sub>3</sub>	H	N	O	2	24	< 5	–
<b>16b</b>	C(CH <sub>3</sub> ) <sub>2</sub> OH	( <i>R</i> )-CH <sub>3</sub>	H	N	NH	13	162	< 5	–

[a] See the Supporting Information for a detailed description of the assay. [b] Aqueous equilibrium solubility at pH 6.8. [c] Values determined in a [<sup>3</sup>H]dofetilide hERG binding assay.

ceptors with higher affinity than **2**. Similarly, **12b** inhibited Hh signaling in a human cell line (HEPM) as measured by the amount of Gli mRNA with an IC<sub>50</sub> ~6-fold lower than that of **2**. Furthermore, **12b** was tested in luciferased C3H10T1/2 cells transfected with a Smo D473H expression vector. Smo D473H is the mutation which conferred resistance to **1** in a medulloblastoma patient after an initial response.<sup>[16]</sup> Remarkably, when tested in this mutant cell line, **12b** retained good potency (IC<sub>50</sub> < 100 nM).<sup>[22]</sup>

**Table 5.** In vivo PK properties of **12b** among preclinical species.

Species	CL <sup>[d]</sup> [mL min <sup>-1</sup> kg <sup>-1</sup> ]	V <sub>ss</sub> <sup>[d]</sup> [L kg <sup>-1</sup> ]	t <sub>1/2</sub> <sup>[d]</sup> [h]	AUC <sub>0-∞</sub> /dose <sup>[e]</sup> μM h/[mg kg <sup>-1</sup> ]	F [%]
mouse <sup>[a]</sup>	21	1.5	1.2	2.83	> 100
rat <sup>[b]</sup>	29	1.6	1.4	0.54	41
dog <sup>[c]</sup>	3	0.5	2.2	10.2	77

[a] Dose: 1 mg kg<sup>-1</sup> i.v., 10 mg kg<sup>-1</sup> p.o., vehicle (i.v., p.o.): 5% NMP/10% PEG400/35% of 10% ETPGS/50% D5W. [b] Dose: 1 mg kg<sup>-1</sup> i.v., 10 mg kg<sup>-1</sup> p.o., vehicle (i.v.): 20% captisol, vehicle (p.o.): 0.5% NaCMC suspension. [c] Dose: 0.1 mg kg<sup>-1</sup> i.v., 0.3 mg kg<sup>-1</sup> p.o., vehicle (i.v., p.o.): 20% captisol. [d] After i.v. dosing. [e] After p.o. dosing.

Compound **12b** shows good bioavailability in preclinical species ranging from 41 to > 100% (Table 5). Systemic plasma clearance (CL) is low (dog and mouse) to moderate (rat), relative to the respective hepatic blood flow, while the volume of distribution at steady state (V<sub>ss</sub>) is low (dog) to moderate (mouse, rat) relative to total body volume. The half-life (t<sub>1/2</sub>) after i.v. dosing ranges from 1.2 to 2.2 h. The compound is able to penetrate the blood–brain barrier as indicated by a brain/plasma AUC<sub>0-∞</sub> ratio of 0.69 after a single dose of 20 mg kg<sup>-1</sup> in mice, which is an important requirement for treating brain tumors.

Next, we determined the efficacy of **12b** in direct comparison against our first-generation inhibitor **2** in a mouse medulloblastoma allograft model. It is well established that mice heterozygous for a loss-of-function mutation in Ptch (Ptch<sup>+/-</sup>) develop medulloblastoma at a frequency of 10–15%.<sup>[23]</sup> Additional heterozygous deletion of the tumor suppressor Hypermethylated in cancer (Hic), a frequent target of epigenetic gene silencing in medulloblastoma, was found to increase the incidence of these tumors fourfold when compared with Ptch<sup>+/-</sup>-only mutants.<sup>[24]</sup> We used medulloblastoma tumors developed spontaneously in Ptch<sup>+/-</sup> Hic<sup>-/-</sup> mice and transferred them subcutaneously to the flank of nude mice. Treatment with Smo antagonists has been shown to result in regression of medulloblastoma in these mice.<sup>[25]</sup> The mice were treated orally with **2** or **12b** for eight days. After this time the vehicle group had to be sacrificed because of excessive tumor size (data not shown for vehicle group). Similarly, the two compounds were assessed using the same Ptch<sup>+/-</sup> Hic<sup>-/-</sup> mouse medulloblastoma tumors but implanted subcutaneously into nude rats. In this case, tumor regression was evaluated after nine days of dosing: the time at which the vehicle group had to be sacrificed because of excessive tumor growth. To develop the PK/efficacy correlation, separate studies in Ptch<sup>+/-</sup> Hic<sup>-/-</sup> medulloblastoma-bearing mice and rats were required with a shorter duration of compound treatment so that sizable tumor remained for analysis of compound exposure. Tumor and plasma samples were collected after different time points after the third dosing to calculate compound exposure described as area under the curves (AUC<sub>0-24h</sub>). As summarized in Table 6, **12b** requires a ~2-fold higher dose than **2** to achieve similar tumor regression in both rodent models. However, **12b** achieved similar ef-

ficacy with a 3–8-fold lower exposure in plasma and tumor as a result of its higher intrinsic potency (see Table 4). The higher dose required for **12b** is a consequence of its shorter half-life in rodents (t<sub>1/2</sub> = 1.2–1.4 h, see Table 5) in comparison with **2** (t<sub>1/2</sub> = 3.9–4.2 h). We also measured inhibition of the Hh pathway in tumors upon treatment with **12b** in Ptch<sup>+/-</sup> Hic<sup>-/-</sup> medulloblastoma-bearing mice. Tumors were harvested at various time points after the third dosing, and expression of Gli1 mRNA as a marker of Hh pathway activity was analyzed. Almost complete

**Table 6.** PK/efficacy relationship for **12b** and **2** in Ptch<sup>+/-</sup> Hic<sup>-/-</sup> rodent models.<sup>[a]</sup>

Species	Dose [mg kg <sup>-1</sup> ] <sup>[b]</sup>	Tumor Regression [%] <sup>[c]</sup>	Tumor Exposure [AUC <sub>0-24h</sub> , μM h] <sup>[d]</sup>	Plasma Exposure [AUC <sub>0-24h</sub> , μM h] <sup>[d]</sup>
<i>Mouse</i>				
<b>12b</b>	40	85	32.1	45.3
<b>2</b>	20	91	259.5	141.5
<i>Rat</i>				
<b>12b</b>	10	98	25.0	30.6
<b>2</b>	5	99	105.3	138.4

[a] See the Supporting Information for detailed study conditions. [b] **12b** was dosed p.o. as a 0.5% NaCMC suspension in water, **2** was dosed p.o. as a diphosphate salt suspension in 0.5% methylcellulose and 0.5% Tween 80 in water; doses expressed as free base equivalent. [c] Tumor regression after eight days of treatment for mice, nine days for rat. [d] Exposure after dosing for three days once daily in separate studies.

(> 90%) and sustained inhibition of Gli1 mRNA over 24 h was observed (Figure 2).

In summary, we have discovered potent Smo inhibitors based on 1-piperazino-4-benzylpyridazines with improved aqueous solubility and decreased activity toward the hERG channel, resulting in compound **12b**. Compound **12b** retains activity against a Smo mutant (D473H) cell line identified in a medulloblastoma patient who had relapsed after an initial response to vismodegib. The compound shows efficacy in subcu-

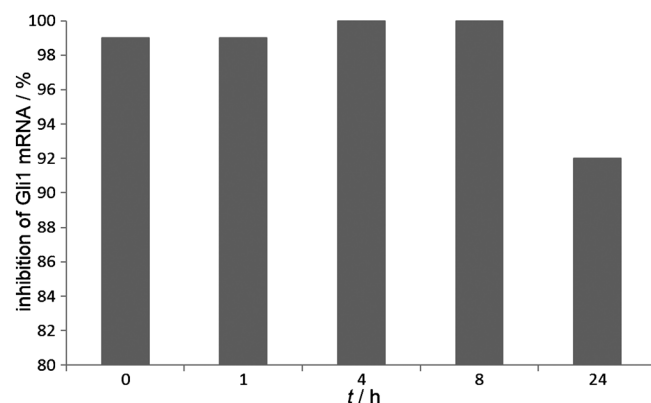


**Figure 2.** Inhibition of Gli1 mRNA expression upon treatment with **12b**. Tumors were harvested 0, 1, 4, 8, and 24 h after dosing 40 mg kg<sup>-1</sup> **12b** p.o. once daily for three days. Gli1 mRNA levels were analyzed by real-time PCR and normalized to β-actin expression. Data are shown as percent inhibition relative to vehicle-treated control tumors.

taneous Ptch<sup>+/-</sup> Hic<sup>-/-</sup> medulloblastoma models in mice and rats, and an analysis of its PK/efficacy relationship demonstrates its high intrinsic potency. This compound is now in clinical development, and its clinical PK, efficacy, and safety are currently under evaluation.

## Experimental Section

Synthetic protocols for all compounds, analytical data, and procedures and methods for in vitro and in vivo assays are available in the Supporting Information. All in vivo research was reviewed and approved by the Novartis Institute of Biomedical Research Institutional Animal Care and Use Committee (IACUC) in accordance with all local, state, and federal regulations.

## Acknowledgements

Authors gratefully acknowledge Dr. Xu Wu and Dr. Shifeng Pan (both Genomics Institute of the Novartis Foundation, La Jolla, California) as well as Dr. Tim Ramsey (NIBR, Cambridge), Dr. Yung-mae Yao, and Dr. Christoph Lengauer for many stimulating discussions throughout the program.

**Keywords:** antitumor agents · hedgehog signaling · medicinal chemistry · pyridazines · smoothed inhibitors

- [1] A. P. McMahon, P. W. Ingham, C. J. Tabin, *Curr. Top. Dev. Biol.* **2003**, *53*, 1–114.
- [2] P. W. Ingham, A. P. McMahon, *Genes Dev.* **2001**, *15*, 3059–3087.
- [3] M. Murone, A. Rosenthal, F. J. de Sauvage, *Curr. Biol.* **1999**, *9*, 76–84.
- [4] L. L. Rubin, F. J. de Sauvage, *Nat. Rev. Drug Discovery* **2006**, *5*, 1026–1033.
- [5] M. P. di Magliano, M. Hebrok, *Nat. Rev. Cancer* **2003**, *3*, 903–911.
- [6] J.-W. Theunissen, F. J. de Sauvage, *Cancer Res.* **2009**, *69*, 6007–6010.
- [7] R. Teperino, S. Amann, M. Bayer, S. L. McGee, A. Loipetzberger, T. Connor, C. Jaeger, B. Kammerer, L. Winter, G. Wiche, K. Dalgaard, M. Selvaraj, M. Gaster, R. S. Lee-Young, M. A. Febbraio, C. Knauf, P. D. Cani, F. Aberger, J. M. Penninger, J. A. Pospisilik, H. Esterbauer, *Cell* **2012**, *151*, 414–426.
- [8] D. D. Von Hoff, P. M. LoRusso, C. M. Rudin, J. C. Reddy, R. L. Yauch, R. Tibes, G. J. Weiss, M. J. Borad, C. L. Hann, J. R. Brahmer, H. M. Howard, B. L. Lum, W. C. Darbonne, J. C. Marsters, Jr., F. J. de Sauvage, J. A. Low, *N. Engl. J. Med.* **2009**, *361*, 1164–1172.
- [9] C. M. Rudin, C. L. Hann, J. Laterra, R. L. Yauch, C. A. Christopher, L. Fu, T. Holcomb, J. Stinson, S. E. Gould, B. Colman, P. M. LoRusso, D. D. Von Hoff, F. J. de Sauvage, J. A. Low, *N. Engl. J. Med.* **2009**, *361*, 1173–1178.
- [10] J. R. Ahnert, J. Baselga, H. A. Tawbi, Y. Shou, C. Granvil, J. Dey, M. M. Mita, A. L. Thomas, D. D. Amakye, A. C. Mita, *J. Clin. Oncol.* **2010**, *28*, 2500.
- [11] For a chemistry-centric review on Smo antagonists, see: S. Peukert, K. Miller-Moslin, *ChemMedChem* **2010**, *5*, 500–512.
- [12] For a review on Smo inhibitors in clinical trials, see: T. L. Lin, W. Matsui, *OncoTargets Ther.* **2012**, *5*, 47–58.
- [13] FDA approval for vismodegib: available at <http://www.cancer.gov/cancertopics/druginfo/fda-vismodegib> [last accessed on June 11, 2013].
- [14] K. D. Robarge, S. A. Brunton, G. M. Castanedo, Y. Cui, M. S. Dina, R. Goldsmith, S. E. Gould, O. Guichert, J. L. Gunzner, J. Halladay, W. Jia, C. Khojasteh, M. F. Koehler, K. Kotkow, H. La, R. L. La Londe, K. Lau, L. Lee, D. Marshall, J. C. Marsters, L. J. Murray, C. Qian, L. L. Rubin, L. Salphati, M. S. Stanley, J. H. A. Stibbard, D. P. Sutherlin, S. Ubhayaker, S. Wang, S. Wong, M. Xie, *Bioorg. Med. Chem. Lett.* **2009**, *19*, 5576–5581.
- [15] S. Pan, X. Wu, J. Jiang, W. Gao, Y. Wan, D. Cheng, D. Han, J. Liu, N. P. Englund, Y. Wang, S. Peukert, K. Miller-Moslin, J. Yuan, R. Guo, M. Matsumoto, A. Vattay, Y. Jiang, J. Tsao, F. Sun, A.-M. C. Pferdekemper, S. Dodd, T. Tuntland, W. Maniara, J. F. Kelleher III, Y. Yao, M. Warmuth, J. Williams, M. Dorsch, *ACS Med. Chem. Lett.* **2010**, *1*, 130–134.
- [16] R. L. Yauch, G. J. P. Dijkgraaf, B. Alicke, T. Januario, C. P. Ahn, T. Holcomb, K. Pujara, J. Stinson, C. A. Callahan, T. Tang, J. Bazan, Z. Kan, S. Seshagiri, C. L. Hann, S. E. Gould, J. L. Low, C. M. Rudin, F. J. de Sauvage, *Science* **2009**, *326*, 572–574.
- [17] A. Sekulic, M. R. Migden, A. E. Oro, L. Dirix, K. D. Lewis, J. D. Hainsworth, J. A. Solomon, S. Yoo, S. T. Aron, P. A. Friedlander, E. Marmor, C. M. Rudin, A. L. S. Chang, J. A. Low, H. M. Macek, R. L. Yauch, R. A. Graham, J. C. Reddy, A. Hauschild, *N. Engl. J. Med.* **2012**, *366*, 2171–2179.
- [18] K. Miller-Moslin, S. Peukert, R. K. Jain, M. A. McEwan, R. Karki, L. Llamas, N. Yusuff, F. He, Y. Li, Y. Sun, M. Dai, L. Perez, W. Michael, T. Sheng, H. Lei, R. Zhang, J. Williams, A. Bourret, A. Ramamurthy, J. Yuan, R. Guo, M. Matsumoto, A. Vattay, W. Maniara, A. Amaral, M. Dorsch, J. F. Kelleher III, *J. Med. Chem.* **2009**, *52*, 3954–3968.
- [19] For a related reaction with pyridazines, see: D. S. Chekmarev, A. E. Stepanov, A. N. Kasatkin, *Tetrahedron Lett.* **2005**, *46*, 1303–1305.
- [20] For a related reaction with pyridazines using copper catalysis, see: D. Peters, G. M. Olsen, E. O. Nielsen, T. D. Jorgensen, D. B. Timmermann (Neurosearch A/S), WO 2005074940, **2005**.
- [21] For a positive correlation between polar surface area and aqueous solubility, see: J. R. Votano, M. Parham, L. H. Hall, L. B. Kier, *Mol. Diversity* **2004**, 379–391.
- [22] Smo antagonist LY-2940680 has been reported to inhibit its activity in C3H10T1/2 cells with IC<sub>50</sub> = 400 nM: M. H. Bender, P. A. Hipskind, A. R. Capen, M. Cockman, K. M. Credille, H. Gao, J. A. Bastian, J. M. Clay, K. L. Lobb, D. J. Sall, M. L. Thompson, T. Wilson, G. N. Wishart, B. K. R. Patel, *102nd Annual Meeting, American Association for Cancer Research*, April 2–6, 2011, Orlando, FL (USA).
- [23] L. V. Goodrich, I. Milenkovic, K. M. Higgins, M. P. Scott, *Science* **1997**, *277*, 1109–1113.
- [24] K. J. Briggs, I. M. Corcoran-Schwartz, W. Zhang, T. Harcke, W. L. Devereux, S. B. Baylin, C. G. Eberhart, D. N. Watkins, *Genes Dev.* **2008**, *22*, 770–785.
- [25] S. Buonamici, J. Williams, M. Morrissey, A. Wang, R. Guo, A. Vattay, K. Hsiao, J. Yuan, J. Green, B. Ospina, Q. Yu, L. Ostrom, P. Fordjour, D. L. Anderson, J. E. Monahan, J. F. Kelleher, S. Peukert, S. Pan, X. Wu, S.-M. Maira, C. Garcia-Echeverria, K. J. Briggs, D. N. Watkins, Y. M. Yao, C. Lengauer, M. Warmuth, W. R. Sellers, M. Dorsch, *Sci. Transl. Med.* **2010**, *2*, 51ra70.

Received: May 15, 2013

Published online on July 2, 2013